Ground State of Two-Dimensional Finite Electron Systems in the Quantum Hall Regime

Henri Saarikoski* and Ari Harju

Laboratory of Physics, Helsinki University of Technology, P.O. Box 1100, FIN-02015 HUT, Finland

(Received 9 March 2005; published 23 June 2005)

We study electronic structures of quasi-two-dimensional finite electron systems in high magnetic fields. The solutions in the fractional quantum Hall regime are interpreted as quantum liquids of electrons and vortices. The ground states are classified according to the number of vortices inside the electron droplet. The theory predicts observable effects due to vortex formation in the chemical potentials and magnetization of electron droplets. We compare the transitions in the theory to those found in electron transport experiments on a quantum dot device and find significant correspondence.

DOI: 10.1103/PhysRevLett.94.246803 PACS numbers: 73.43.−f, 71.10.−w, 73.21.La, 85.35.Be

Studies of finite two-dimensional electron systems in high magnetic fields often get their inspiration from the remarkable physics of the quantum Hall effect in two-dimensional electron gas [1]. Considerable experimental and theoretical work has been carried out, in particular, on quantum dots, two-dimensional droplets of electrons in the interface region of semiconductor heterostructures [2–5]. Electron transport measurements of quantum dots have revealed a rich variety of transitions associated with charge redistribution within the electron droplet in high magnetic fields [6]. This has led to the development and study of theoretical models which could account for the microscopic origin of these phenomena [7–10]. Recently a proposal has been put forth that the observed phenomena may be caused by the emergence of a special state of electronic matter, a quantum liquid of strongly correlated electrons and vortices [11–14]. In the present work we use this approach to classify the ground states of the two-dimensional electron droplets in quantum dots and compare transitions to those found in electron transport measurements. Our results give also general insight into the internal structure of the many-body wave function of finite two-dimensional electron systems.

Vortices, rotational flow of currents or matter with a characteristic cavity at the center, can be found in various natural phenomena where particles have been set to rotate around a common axis. Descriptions of vortices exist since antiquity [15]. In two-dimensional quantum systems a vortex can be defined in analogue with classical vortices as a zero in the wave function associated with a phase change of the integer multiple of 2π for each path enclosing this zero. In quantum dots the rotation of electrons is induced by external magnetic field and vortices may form if this rotation is strong. Vortices are caused by quantization of the magnetic flux through the electron droplet, and they give rise to rotating currents of charge around density zeros inside the electron droplet. Vortices create charge deficiency inside the electron droplet which manifests itself as an increase of the dot area [7,8]. This theory has been based on electronic structure studies of quantum dots [11,13,14] as well as on theoretical analogies with bosonic systems of rotating Bose-Einstein condensates [12]. Vortices in electron droplets are not necessarily bound to electrons as approximated by the Laughlin wave functions. The analysis of the internal structure of the many-body wave function suggests the introduction of a more general framework of an interacting system of electrons and off-electron vortex quasiparticles, where vortex formation is driven by interactions [14,16].

We use an effective-mass approximation in the xy plane to model the physics of a quasi-two-dimensional system of trapped electrons in vertical quantum dot devices. The electron-electron interaction is approximated with a Coulomb potential. The Hamiltonian is then

$$H = \sum_{i=1}^{N}\left(\frac{(-i\hbar\nabla_i + e\mathbf{A})^2}{2m^*} + V_{\mathrm{c}}(r_i)\right) + \frac{e^2}{4\pi\epsilon}\sum_{i<j}\frac{1}{r_{ij}}, \quad (1)$$

where N is the number of electrons, V_{c} is the external confining potential, m^* is the effective mass of electrons moving in a semiconductor medium, ϵ is the dielectric constant, and $\mathbf{A}$ is the vector potential of the homogeneous magnetic field which is oriented perpendicular to the xy plane. In the subsequent discussion the external potential is chosen to be parabolic $V_c(r) = \frac{1}{2}m^*\omega_0^2 r^2$.

In this Letter we use both the mean-field spin-density-functional theory (SDFT) and the variational quantum Monte Carlo (VMC) method to calculate the electronic structure in the quantum Hall regime. We use the SDFT in conjunction with local spin density approximation (LSDA) with a smooth correlation functional [17]. For details of the implementations we refer to Refs. [11,18]. In high magnetic fields the electron droplet is spin polarized and a stable structure called the maximum density droplet (MDD) forms [19]. It is a finite-size precursor of the integer $\nu = 1$ quantum Hall state. Evidence for the MDD formation has been reported in the experiments [5,6]. When the magnetic field is increased in the measurements, the MDD breaks down into a lower density droplet in the fractional quantum Hall (FQH) regime.

Theory predicts that in parabolically confined quantum dots the ground states in the beyond-MDD (FQH) regime occur only at certain ''magic'' angular momentum values

[20]. As a result, the angular momentum as a function of the external magnetic field shows a characteristic staircase structure. In the MDD breakdown the angular momentum increase with respect to the MDD state $\Delta L = L - L(\mathrm{MDD})$ strongly depends on the number of electrons in the system [18]. For $N \leq 12$ the electron in the center is moved to the outer edge giving $\Delta L = N$ and a vortex hole emerges at the center of the dot. For $N > 12$ a vortex emerges at a finite distance from the center [8]. This change in the breakdown mechanism means that vortices in large electron systems tend not to localize. However, if the symmetry of the external potential is broken, localized vortices may form in the particle and current densities [14]. High angular momentum states correspond to multivortex configurations in the FQH regime. Since they are beyond reach for exact diagonalization techniques for $N > 10$, we use the SDFT to analyze the electronic structure of these states.

In the experimental realizations of quantum dots the area of the dot has been found to increase with the gate voltage, suggesting that the electron density in the dot remains constant [21]. In zero magnetic field this implies a confining potential that scales as $\hbar\omega_0 \sim N^{-1/4}$ [22]. However, the magnetic field exerts an additional squeezing effect on the electrons, which is counteracted by interactions. We have found that approximately constant electron density in the calculations is obtained by a potential scaling $\hbar\omega_0 \sim N^{-1/7}$. Figure 1 shows phase diagrams of the ground states in the SDFT. The ground states are classified according to the number of vortices inside the electron droplet by using conditional single-determinant wave functions constructed from Kohn-Sham orbitals [23].

For qualitative understanding of the structure of the phase diagram we interpret the solutions in the FQH domain as a quantum liquid of electrons and holelike vortex quasiparticles. The MDD state assigns one Pauli vortex at each electron position. As the MDD reconstructs the number of vortices in the system increases by one and subsequent transitions involve the emergence of more off-electron vortices. Since vortices carry magnetic flux quanta Φ_0, the MDD state breaks down approximatively when the magnetic flux $\Phi = BA$ through the MDD of area A exceeds $(N+1)\Phi_0$ and an additional off-electron vortex emerges in the electron droplet. The compactness of the MDD state and the observed constancy of the electron density n with respect to N gives $N = nA$ and $B = (1 + 1/N)\Phi_0 n$ for the MDD reconstruction. The upper boundary of the MDD is therefore approximatively constant for high N in accord with the experiments [6]. With the addition of one vortex in the MDD the relative increase of the dot area is approximately $1/N$. This increase of the dot area via vortex formation counteracts the squeezing effect of the magnetic field. Assuming now a constant n for the beyond-MDD states, the change in required for the addition of subsequent off-electron vortices in the droplet is approximately $\Delta B = \Phi_0 n/N$. The calculations show that widths of the different vortex phases are to a good accuracy inversely proportional to N which gives credence to this simplified picture [see Fig. 1(b)]. The above reasoning implies also that constancy of the electron density in the droplet leads to narrowing of the MDD window for high electron numbers. The lower boundary of the MDD is determined from either polarization of the electron droplet or the flipping of one vortex from parallel to antiparallel orientation with respect to the magnetic field. The latter condition involves a constant flux change of $2\Phi_0$ with respect to the MDD state. This leads to narrowing of the MDD window because the area of the droplet increases with N in a totally polarized system. However, for realistic Zeeman-coupling strengths the electron droplet loses total

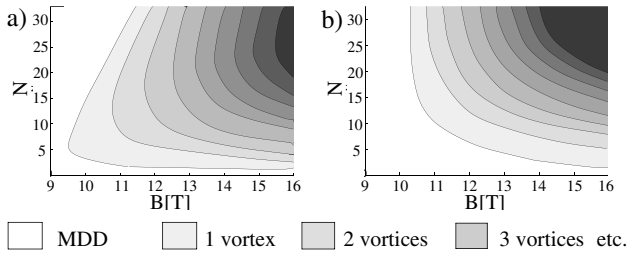

FIG. 1. Mean-field SDFT phase diagrams of the ground state of parabolically confined electron droplets in high magnetic fields. The ground states are classified according to the number of vortices inside the electron droplet (gray scale). The confining potential is $\hbar\omega_0 = 5$ meV in (a) and $7.67N^{-1/7}$ meV in (b). In the upper right hand corner of the right diagram the number of vortices is greater than 8.

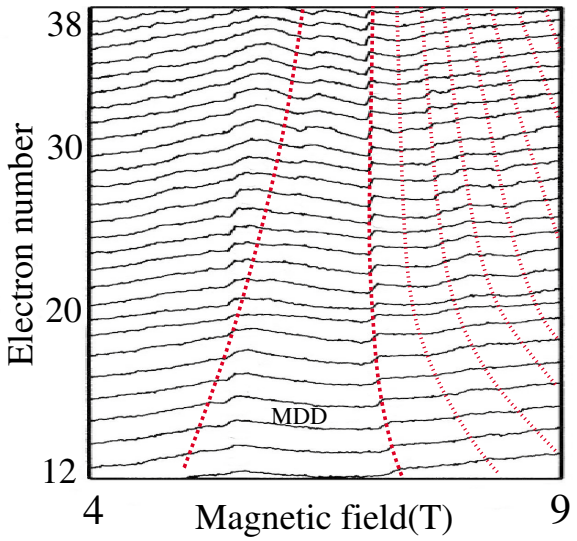

FIG. 2 (color online). Current peaks in the electron transport experiments and transitions in the SDFT (red lines). The dashed lines denote the MDD boundaries. The right dashed line and the dotted lines correspond to transitions associated with the emergence of off-electron vortices one by one inside the electron droplet. The experimental data are from Fig. 2b in Ref. [6].

spin polarization in the low-field limit before antivortices emerge. This shrinks the MDD window further.

We now compare these theoretical results with experimental data from electron transport measurements. Oosterkamp and co-workers measured electron transport through a vertical quantum dot device in the quantum Hall regime [6]. Up to this date these experiments give the best available electron transport data for a single-dot device. Figure 2 shows chemical potentials in these experiments for electron numbers $N = 12$ to 39, the MDD window boundaries in the SDFT as well as the transitions associated with the emergence of off-electron vortices. The gate voltage dependence of the external confinement in the quantum dot device is taken into account by using confining potential $\hbar\omega_0 = 5.70N^{-1/7}$ meV in the SDFT. For material parameters we use $m^* = 0.067$, $\epsilon = 12.4$, and effective gyromagnetic ratio $g^* = -0.44$. Despite the simple form of the interelectron potential in our theoretical model, the transitions in the beyond-MDD domain fit well into the experimental data. This can be understood from the fact that the transitions are induced by the magnetic flux quantization through the relatively compact electron droplet. In Fig. 3 the chemical potential of the 24-electron quantum dot is calculated with the SDFT, the VMC simulation, and the exact diagonalization in the lowest Landau level (LLL). The results are compared to the experimental data in Ref. [6]. The correspondence between the theory and experiments is good, and different quantum Hall regimes can be identified by comparing the two sets of data. We find also that the theoretical results are consistent with the observed narrowing of the MDD window from about 1 T at $N = 20$ to 0.5 T at $N = 39$ (see Fig. 2). In the SDFT

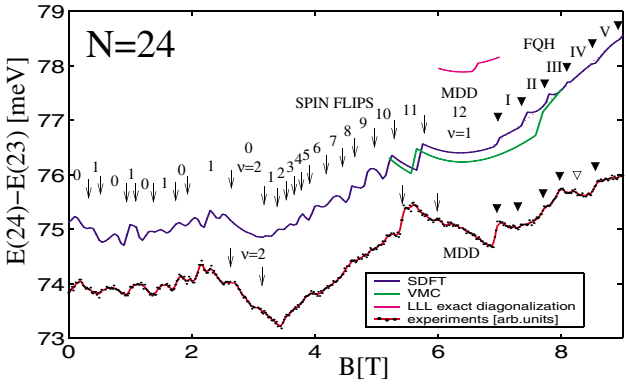

FIG. 3 (color online). Chemical potential of the 24-electron quantum dot calculated with the SDFT and compared to the experiments from Ref. [6] and VMC and LLL exact diagonalization results in the vicinity of the MDD window. Noise in the experimental data has been reduced by using a Gaussian filter. The numbers between the arrows indicate the total spin. The roman numbers between the triangles indicate the number of vortices inside the electron droplet in the fractional quantum Hall regime. Charge-density-wave solutions in the SDFT (dotted line) have been discarded as unphysical.

the partially polarized states in the spin-flip region have a MDD-like compact structure for both orientations of the z component of the spin. Therefore the states before the MDD around 6 T for high N in Fig. 2 could be partially polarized states, and the MDD window may be smaller than that identified in Ref. [6]. In theory the increase in the dot area at the MDD breakdown is approximately $1/N = 3.3\%$ at $N = 30$. This can be contrasted to around 10% reported in the experiments [6]. However, uncertainty in the experimental result is high, and there exists no analysis of a possible N dependence [24].

The electron transport data show features that may be due to correlation effects beyond our mean-field SDFT. These may include the transition associated with the open triangle in Fig. 3 and fluctuations in the data between the second and third triangles. In addition, the LLL theory of Ref. [9] suggests that for small particle numbers (≤ 100), the first ground state after MDD would have partial spin polarization. However, higher Landau levels might have an effect on this [25]. In actual quantum dot realizations, effects due to finite thickness of the electron gas, screening of the interaction potential, image charges, and nonparabolic terms in the external potential may also cause deviations from our results [26].

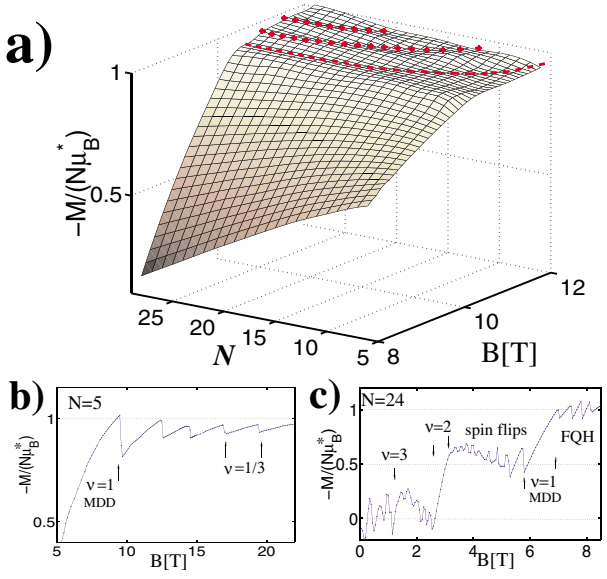

FIG. 4 (color online). (a) Ground state magnetization per electron calculated with the SDFT. The confining potential is $7.67N^{-1/7}$ meV. The beyond-MDD states are characterized by a plateau region in this plot, where magnetization per electron is close to μ_B^*. The dashed and the dotted lines correspond to the same transitions as in Fig. 2. (b),(c) Detail plots of the oscillations in the magnetization of the 5-electron and 24-electron droplets, respectively. The finite-size precursor of the $\nu = 1/3$ quantum Hall state is identified by using conditional wave functions [11]. The confinement strength is 5 meV in (a) and 3.62 meV in (b). The oscillations in plot (a) are smoothed out due to use of finite temperature.

In the electron transport experiments the slope of the chemical potential is the magnetization difference $M(N, B) - M(N-1, B)$, where $M = -\partial E/\partial B$. Since the magnetic field couples to the angular momentum L, there is a jump in the magnetization at transitions associated with change in L. In the MDD state the angular momentum increases with N as $N \rightarrow N+1$. Therefore the slopes of the chemical potentials in the MDD domain show a typical decreasing pattern as N increases at fixed B. SDFT calculations indicate that magnetization per electron in the FQH regime is close to the effective Bohr magneton $\mu_{\mathrm{B}}^{*} = m_e/m^{*}\mu_{\mathrm{B}} = 0.864$ meV/T (see Fig. 4). This is a consequence of the emergence of additional vortex quasiparticles in the electron droplet as the magnetic field increases. This behavior gives rise to positive slopes in the chemical potentials in the beyond-MDD domain which is in accord with experimental data (see, e.g., slopes of the chemical potentials at $B = 9$ T in Fig. 2). Detail plots of the magnetization for $N = 5$ and $N = 24$ in the mean-field theory [Figs. 4(b) and 4(c)] reveal also oscillations in the droplet magnetization as the number of vortices increases one by one [14]. The sawtoothlike oscillations in lower magnetic fields in Fig. 4(c) are manifestations of the de Haas–van Alphen effect. The overall behavior is similar to that found in direct measurements of magnetization of dot mesas [27]. This method could also provide a way to detect oscillations in the FQH regime.

To conclude, we have performed theoretical calculations for finite electron droplets in the quantum Hall regime. Our model theory predicts the emergence of a quantum liquid of electrons and off-electron vortices in high magnetic fields. The pattern of transitions found within the theory is consistent with experimental data from electron transport measurements. However, for greater qualitative understanding of the phenomena, we call for more accurate electron transport experiments in the quantum Hall regime, more accurate computational methods, and more realistic modeling of quantum dot systems in the case of many-electron systems. It has been suggested that the addition of cusps to smooth LSDA functionals incorporates more FQH correlations [28]. Another approach towards testing of the validity of theoretical predictions could be a direct visualization of the electron density in a quantum dot. Recent developments with scanned probe imaging techniques [29,30] could yield a way to image localized vortices in electron droplets.

We are grateful to the authors of Ref. [6] for permission to reproduce some of the published electron transport data. We thank E. Räsänen, S. M. Reimann, L. Kouwenhoven, D. G. Austing, Y. Nishi, M. Marlo-Helle, G. S. Jeon, and M. Puska for fruitful discussions and K. Saloriutta for computational work in producing Fig. 4(b). This work has been supported by the Academy of Finland through the Centre of Excellence Program (2000–2005).

*Electronic address: hri@fyslab.hut.fi

[1] T. Chakraborty and P. Pietiläinen, *The Quantum Hall Effects: Fractional and Integral* (Springer, Berlin, 1995).
[2] L. Jacak, P. Hawrylak, and A. Wójs, *Quantum Dots* (Springer, Berlin, 1998).
[3] L. P. Kouwenhoven and C. M. Marcus, Phys. World **11**, 35 (1998).
[4] S. M. Reimann and M. Manninen, Rev. Mod. Phys. **74**, 1283 (2002).
[5] R. C. Ashoori, Nature (London) **379**, 413 (1996).
[6] T. H. Oosterkamp, J. W. Janssen, L. P. Kouwenhoven, D. G. Austing, T. Honda, and S. Tarucha, Phys. Rev. Lett. **82**, 2931 (1999).
[7] S. M. Reimann, M. Koskinen, M. Manninen, and B. R. Mottelson, Phys. Rev. Lett. **83**, 3270 (1999).
[8] S.-R. Eric Yang and A. H. MacDonald, Phys. Rev. B **66**, 041304(R) (2002).
[9] J. H. Oaknin, L. Martín-Moreno, and C. Tejedor, Phys. Rev. B **54**, 16 850 (1996).
[10] P. A. Maksym, H. Imamura, G. Mallon, and H. Aoki, J. Phys. Condens. Matter **12**, R299 (2000).
[11] H. Saarikoski, A. Harju, M. J. Puska, and R. M. Nieminen, Phys. Rev. Lett. **93**, 116802 (2004).
[12] M. Toreblad, M. Borgh, M. Koskinen, M. Manninen, and S. M. Reimann, Phys. Rev. Lett. **93**, 090407 (2004).
[13] M. B. Tavernier, E. Anisimovas, and F. M. Peeters, Phys. Rev. B **70**, 155321 (2004).
[14] H. Saarikoski, S. M. Reimann, E. Räsänen, A. Harju, and M. J. Puska, Phys. Rev. B **71**, 035421 (2005).
[15] Charybdis is described as a giant whirlpool in Homer's epic poem the Odyssey, book XII.
[16] M. Manninen, S. M. Reimann, M. Koskinen, Y. Yu, and M. Toreblad, Phys. Rev. Lett. **94**, 106405 (2005).
[17] C. Attaccalite, S. Moroni, P. Gori-Giorgi, and G. B. Bachelet, Phys. Rev. Lett. **88**, 256601 (2002).
[18] Ari Harju, cond-mat/0505053 [J. Low Temp. Phys. (to be published)].
[19] A. H. MacDonald, S.-R. Eric Yang, and M. D. Johnson, Aust. J. Phys. **46**, 345 (1993).
[20] T. Seki, Y. Kuramoto, and T. Nishino, J. Phys. Soc. Jpn. **65**, 3945 (1996).
[21] Guy Austing *et al.*, Jpn. J. Appl. Phys. **38**, 372 (1999).
[22] M. Koskinen, M. Manninen, and S. M. Reimann, Phys. Rev. Lett. **79**, 1389 (1997).
[23] H. Saarikoski, A. Harju, M. J. Puska, and R. M. Nieminen, Physica (Amsterdam) **26E**, 317 (2005).
[24] Guy Austing (private communication).
[25] S. Siljamäki, A. Harju, R. M. Nieminen, V. A. Sverdlov, and P. Hyvönen, Phys. Rev. B **65**, 121306(R) (2002).
[26] Y. Nishi, P. A. Maksym, D. G. Austing, T. Hatano, L. P. Kouwenhoven, H. Aoki, and S. Tarucha (to be published).
[27] M. P. Schwarz, D. Grundler, Ch. Heyn, D. Heitmann, D. Reuter, and A. Wieck, Phys. Rev. B **68**, 245315 (2003).
[28] M. I. Lubin, O. Heinonen, and M. D. Johnson, Phys. Rev. B **56**, 10 373 (1997).
[29] Mark A. Topinka, Robert M. Westervelt, and Eric J. Heller, Phys. Today **56**, No. 12, p. 47 (2003).
[30] P. Fallahi *et al.*, Nano Lett. **5**, 223 (2005).